Binary and ternary mixed metal complexes of terminally free peptides containing two different histidyl binding sites

Ágnes Grenács[a], Anikó Kaluha[a], Csilla Kállay[b], Viktória Jószai[a], Daniele Sanna[c], Imre Sóvágó*[,a]

[a] *Department of Inorganic and Analytical Chemistry, University of Debrecen, H-4010 Debrecen, Hungary*

[b] *Research Group of Homogeneous Catalysis and Reaction Mechanism, Hungarian Academy of Sciences, H-4010 Debrecen, Hungary*

[c] *Istituto di Chimica Biomolecolare, CNR, Traversa La Crucca 3, Regione Baldinca, 07040 Li Punti (SS), Italy*

Abstract

Copper(II), nickel(II) and zinc(II) complexes of the terminally free peptides AHAAAHG and AAHAAAHG have been studied by combined applications of potentiometric and various spectroscopic techniques, including UV-visible, CD and EPR for copper(II) and UV-visible, CD and NMR for nickel(II). It was found that the octapeptide AAHAAAHG can easily bind two equivalents of copper(II) or nickel(II) ions and the amino terminus was identified as the primary ligating site of the molecule. On the other hand, this peptide has a relatively low zinc(II) binding affinity. Mono- and di-nuclear copper(II) and nickel(II) complexes were also formed with the heptapeptide AHAAAHG but this peptide can effectively bind one equivalent of zinc(II) ions, too, with the involvement of the deprotonated amide nitrogen in zinc(II) binding. The enhanced stability of the $[MH_{-1}L]$ species of AHAAAHG was explained by the tridentate (NH_2,N^-,N_{im}) coordination of the amino terminus supported by the macrochelation of the internal histidyl residue. Mixed metal copper(II)-nickel(II) complexes were also formed with both peptides and copper(II) ions were coordinated to the amino terminal, while nickel(II) ions to the internal histidyl sites.

Keywords:

copper(II), nickel(II), zinc(II), peptides, histidine, stability constants

* Corresponding author: Tel.: +36 52 512900/22303; Fax: +36 52 518660, E-mail: sovago@science.unideb.hu

1. Introduction

Histidyl residues are well known as the most common binding sites of various metalloproteins and metalloenzymes. The presence of histidine in the proteins responsible for the development of various neurodegenerative disorders (or conformational diseases) promoted further studies on the metal complexes of multihistidine peptides. Huge number of papers has been published on this subject in the last two decades reflecting the great variety of the complex formation processes of these ligands. It cannot be the aim of this paper to give a complete overview of these studies but the readers can easily find the most important results in several recent reviews [1-6]. It is evident from these compilations that the metal binding ability of the peptides largely depends on the number and location of histidyl residues in the sequence. The enhanced copper(II) and nickel(II) binding affinity of the albumin-like amino termini (Xaa-Yaa-His…) has already been well documented for a series of small peptides [1,3,6,7]. The specific coordination modes of the N-terminal histidyl residues and also the Xaa-His sequences have also been satisfactorily clarified [1,3,6]. The studies on the copper(II) complexes of the peptide fragments of prion protein and related substances revealed that the internal histidyl residues can also be anchoring sites for copper(II) or nickel(II) binding [5]. Moreover, the formation of polynuclear copper(II) and/or nickel(II) complexes was observed with various multihistidine peptides [8-11]. Peptide fragments of prion protein and amyloid-β peptides provided the most evident examples for the binding of more than one copper(II) and nickel(II) ions in these complexes [12-16]. It was also clear from these studies that the metal ion affinities of the various histidyl sites are not equivalent and a series of coordination isomers of the mononuclear complexes can be present in solution [5,16].

The studies on the copper(II) and nickel(II) complexes of the peptide fragments of prion protein revealed that even the presence of the non-coordinating side chain residues can significantly influence the ratio of coordination isomers. Moreover, it turned out that the distribution of the metal ions among the various binding sites very much depends on the nature of metal ions and a completely different saturation of the specific sites was obtained for copper(II) and nickel(II) ions [5]. These observations promoted the launch of systematic studies on the mixed metal complexes of various multihistidine peptides. The preliminary studies in this field involved the complexes of simple multihistidine model peptides [17] and various fragments of prion protein [18,19] and amyloid-β peptide [20,21]. On the other hand, the comparison of the metal binding affinities of the different coordination modes created by histidyl residues is also crucial for the determination of the favoured coordination isomers. These data are now available for the small peptides containing one histidyl residue in different environments, but no reliable comparison is possible when the different coordination modes exists in one peptide molecule. Now in this paper we report the synthesis of two, terminally free model peptides containing two separate histidyl residues and the studies on their binary copper(II), nickel(II), zinc(II) and ternary or mixed metal complexes with the same metal ions. The heptapeptide AHAAAHG provides a good chance for the comparison of the tridentate (NH_2,N^-,N_{im}) and the tetradentate (N_{im},$3N^-$) coordination modes, while in the case of the octapeptide AAHAAAHG, the albumin-like (NH_2,$2N^-$,N_{im}) and the internal (N_{im},$3N^-$) coordination environments can be compared. Scheme 1 is used to compare these major binding modes of the peptides of histidine.

Scheme 1

2. Experimental

2.1. Peptide synthesis and other materials

The terminally free peptides NH_2-AlaHisAlaAlaAlaHisGly-OH (AHAAAHG) and NH_2-AlaAlaHisAlaAlaAlaHisGly-OH (AAHAAAHG) were synthesized by means of a Liberty 1 solid phase peptide synthesizer using the Fmoc technique. All solvents and chemicals used for synthesis were obtained from commercial sources in the highest available purity and used without further purification. Both N-fluorenylmethoxycarbonyl (Fmoc)-protected amino acids (Fmoc-His(Trt)-OH and Fmoc-Ala-OH,) and 2-(1-H-benzotriazole-1-yl)-1,1,3,3-tetramethyluronium tetrafluoroborate (TBTU) were from Novabiochem (Switzerland), while the Fmoc-Gly-Wang resin was Merck product. Peptide-synthesis grade N,N-dimethylformamide (DMF), N,N-diisopropyl-ethylamine (DIEA), 1,2-ethanedithiol and trifluoroacetic acid (TFA) were purchased from Merck Kft. 1-hydroxybenzotriazole hydrate ($HOBt \cdot H_2O$), N-methyl-pyrrolidone (NMP), triisopropylsilane (TIS), 2,2'-(ethylenedioxy)diethanethiol, diethyl ether (Et_2O) and 2-methyl-2-butanol were Sigma-Aldrich products. Piperidine and dichloromethane (DCM) were Molar solvents as well as acetonitrile (ACN) and acetic anhydride were from VWR.

In case of both peptides solid phase peptide synthesis was performed using a microwave-assisted Liberty 1 Peptide Synthesizer (CEM, Matthews, NC), introducing the amino acid derivatives following the TBTU/HOBt/DIEA activation strategy on the Fmoc-Gly-Wang resin. Removal of the Fmoc was carried out at 75 °C with 35 Watts microwave power for 180 s by means of 20% piperidine in DMF. Coupling was achieved at 75 °C with 25 Watts microwave power, for 300 s, using 4 times amino acids excess, 0.5 M HOBt/0.5 M TBTU in DMF and 2 M DIEA in NMP. Finally, the N-terminal Fmoc group was removed as mentioned before. Peptides were cleaved from their respective resins, with the simultaneous

removal of the side chain protective groups, by treatment with a mixture of TFA/TIS/H_2O/ 2,2'-(ethylenedioxy)diethanethiol (94/2.5/2.5/1 v/v) for 1.5 h at room temperature. Each solution containing the free peptide was separated from the resin by filtration. The crude peptides were recovered from the pertinent solution by precipitation with cold dinethyl ether. The precipitate was washed with cold diethyl ether and separated from it, than dried, redissolved in water, and finally lyophilized. The purity of the peptides was checked by analytical rp-HPLC analyses using a Jasco instrument, equipped with a Jasco MD-2010 plus multiwavelength detector. The analyses were performed by eluting solvent A (0.1% TFA in acetonitrile) and solvent B (0.1% TFA in water) on a Vydac C18 chromatographic column (250 x 4.6 mm, 300 Á pore size, 5 μm particle size) at a flow rate of 1 mL/min, 3% of solvent B monitoring the absorbance at 222 nm. The purity of the peptides was checked by HPLC and by recording the pH-dependent ^{1}H NMR spectra of the peptides. Potentiometric titrations also confirmed the purity and the identity of the peptides. For all peptides the purity was greater than 94%.

The metal ion stock solutions were prepared from analytical grade reagents of $CuCl_2$, $NiCl_2$ and $ZnCl_2$ and their concentrations were checked by gravimetry via the precipitation of oxinates.

2.2. Potentiometric measurements

The pH-potentiometric titrations were performed in 3 mL samples at 2 mM ligand concentration with the use of carbonate-free stock solution (0.2 M) of potassium hydroxide. The metal ion to ligand ratios were selected as 1:1 and 2:1 for binary systems and 1:1:1 for ternary systems. The 1.5:1 ratio was also included for the copper(II) and nickel(II)-AHAAAHG system to avoid precipitation. The copper(II) and zinc(II) complexes were formed in fast reactions while the equilibration of the nickel(II)-peptide systems required a

few minutes for each titration points. This is reflected in the increased standard deviations of stability constants of the nickel(II) complexes. During the titration, argon was bubbled through the samples to ensure the absence of oxygen and carbon dioxide. The samples were stirred by a VELP Scientific magnetic stirrer. All pH-potentiometric measurements were carried out at 298 K and at a constant ionic strength of 0.2 M KCl. pH measurements were made with a MOLSPIN pH-meter equipped with a 6.0234.100 combination glass electrode (Metrohm) and a MOL-ACS microburette controlled by a computer. The recorded pH readings were converted to hydrogen ion concentration. Protonation constants of the ligands and overall stability constants (log β_{pqrs}) of the metal complexes were calculated by means of the general computational programs, (PSEQUAD and SUPERQUAD) as described in our previous publications [19,20]. The equilibrium constants were defined by equations (1) and (2) for the binary and (3) and (4) for the ternary systems.

$$pM + qH + rL = M_pH_qL_r \quad (1)$$

$$\beta_{pqr} = \frac{[M_pH_qL_r]}{[M]^p \cdot [H]^q \cdot [L]^r} \quad (2)$$

$$pCu + qNi + rH + sL = Cu_pNi_qH_rL_s \quad (3)$$

$$\beta_{pqrs} = \frac{[Cu_pNi_qH_rL_s]}{[Cu]^p \cdot [Ni]^q \cdot [H]^r \cdot [L]^s} \quad (4)$$

2.3. Spectroscopic measurements

UV-visible spectra of the copper(II) and nickel(II) complexes were recorded from 250 to 800 nm on a Perkin Elmer Lambda 25 scanning spectrophotometer in the same concentration range as used for pH-potentiometric measurements.

CD spectra of the same complexes were recorded on a JASCO J-810 spectropolarimeter using 1 and/or 10 mm cells in the 220-800 nm wavelength range at the same concentration as used for pH-potentiometry.

Frozen solution EPR spectra were recorded on a Bruker EMX spectrometer, equipped with a HP 53150A microwave frequency counter, at 120 K. Copper(II) stock solutions for EPR measurements were prepared from $CuSO_4 \cdot 5H_2O$ that had been enriched with ^{63}Cu to achieve better resolution of EPR spectra. Metallic copper (99.3% ^{63}Cu and 0.7% ^{65}Cu) was purchased from JV Isoflex (Moscow, Russia) for this purpose and was converted into the sulfate. Ethylene glycol (10%) was added to the aqueous copper(II) complex solutions to increase resolution and to avoid the aggregation processes.

Nuclear magnetic resonance (^1H-NMR) spectra of the nickel(II)-peptide complexes and the free ligands were recorded at c_L = 0.01 M on a Bruker AM 360 MHz FT-NMR spectrometer using tetramethylammonium tetrafluoroborate as an internal standard (3.18 ppm).

ESI-TOF-MS analysis was carried out with a Bruker micrOTOF-Q 9 ESI-TOF instrument in the negative mode. The measurements were performed in water at $c_L=1\times10^{-4}$ M at Cu(II):Ni(II):L = 0.9:0.9:1 ratio at pH=10.3 by adding 0.2 M KOH solution. Temperature of drying gas (N_2) was 180 °C. The pressure of the nebulizing gas (N_2) was 0.3 bar. The capillary voltage applied was 4000 V. The spectra were accumulated and recorded by a digitalizer at a sampling rate of 2 GHz.

3. Results and discussion

3.1. Speciation and structure of the copper(II), nickel(II) and zinc(II) complexes of the terminally free octapeptide AAHAAAHG

Fully protonated form of the octapeptide contains four dissociable protons and the corresponding pK values are listed in Table 1 together with the stability constants of the metal complexes. The deprotonation of the carboxylic function occurs in the acidic pH range and this process is well separated from those of the nitrogen donors. The pH-dependent NMR spectra of the ligand unambiguously reveal that the terminal amino group is the most basic site of the peptide, while the deprotonation of the histidyl sites takes place in overlapping processes. Similar observations have already been reported for a series of other simple multihistidine peptides [22].

Table 1

The presence of a terminal amino group and two histidyl residues offer the possibility of two well separated metal binding sites in this peptide. The amino terminus with His(3) residue corresponds to an albumin-like binding site, while His(7) can be the other anchoring group for metal ion coordination. In agreement with this expectation the formation of both mono- and di-nuclear complexes was observed with copper(II) and nickel(II) ions, while only mononuclear species were formed with zinc(II). The octapeptide was not able to keep two equivalents of zinc(II) ions in solution and the formation of zinc(II)-hydroxide precipitate was observed in slightly alkaline samples. The formation of three species $[ZnHL]^{2+}$, $[ZnL]^{+}$ and $[ZnH_{-1}L]$ were obtained in the pH range from 5.0 to 8.0 from the computer evaluation of the potentiometric measurements. The stability constant of the species $[ZnL]^{+}$ is just between the values reported for the 2N-and 3N-coordinated macrochelates [23] supporting the existence of various coordination isomers in which the terminal amino and one or two imidazole-N can be

involved in metal binding. These binding modes can keep zinc(II) in solution at neutral pH but it is followed by hydrolytic processes and precipitation by increasing pH. These data support previous observations that neither the albumin-like binding sites nor internal histidyl residues can promote the involvement of amide nitrogens in zinc(II) binding of peptides [24,25]. On the other hand, the formation of bis(ligand) complexes cannot be ruled out with the involvement of the amino terminus but the concentration of these species was too low for detection under our experimental conditions.

The speciation curves of the 1:1 and 2:1 copper(II)-AAHAAAHG systems are shown in Figure 1 indicating the formation of dinuclear species in the 2:1 samples and the outstanding copper(II) binding ability of the ligand. The speciation curves of the corresponding nickel(II) containing systems (see Figure S1 in the Supplement) are very similar to those of copper(II) but the complex formation is shifted to the higher pH range (1.5-2.0 pH units). This difference is also reflected in the lower stability constants of the nickel(II) species in Table 1. The easy formation of dinuclear species in the presence of excess metal ions definitely proves the involvement of both potential binding sites in metal ion coordination. The preferred binding site of the mononuclear species, however, cannot be determined from the potentiometric data. On the other hand, the high similarity in the speciation of the two metal ions suggests the existence of the same or rather similar coordination modes in their complexes. Spectroscopic measurements made it possible to determine these binding modes and to clarify the preferred binding sites for the mononuclear species.

Figure 1

EPR spectra of frozen solutions and the visible absorption and circular dichroism spectra of the 1:1 and 2:1 copper(II)-AAHAAAHG samples (see Figures S2 to S4 in

Supplement) have been recorded as a function of pH. The spectral parameters of the major species are recorded in Table 2. It is clear from Table 2 that the two major species of the equimolar samples have the same spectral parameters. Both the absorption and EPR spectra strongly support the coordination of four nitrogen donors in these species suggesting the exclusive binding of copper(II) ions to the N-terminus of the peptide in the (NH_2,$2N^-$,N_{im}) coordination mode. The two species [$CuH_{-1}L$], or [$CuH_{-2}L(H)$], and [$CuH_{-2}L]^-$, differ for the deprotonation degree of the uncoordinated His(7). The pK of deprotonation of the histidyl residue in [$CuH_{-1}L$], 6.94, is very similar to that of the free ligand, 6.88. The binding of copper(II) to the internal histidyl site should be accompanied by the deprotonation of three amide groups but the species $[CuH_{-3}L]^{2-}$ cannot be detected even at very high pH values. The results of equilibrium calculations in a model system led to similar conclusions. The tetrapeptides NH_2-MKHM and Ac-MKHM were considered in these calculations which can form the (NH_2,$2N^-$,N_{im}) and ($3N^-$,N_{im}) coordination modes in separate molecules [25]. It was found that in a sample containing the three components in equimolar concentrations, more than 99 % of copper(II) ions are bonded to the $[CuH_{-2}L]^-$ species of the N-terminally free tetrapeptide, while the ratio of copper(II) present in the $[CuH_{-3}L]^{2-}$ species of the terminally protected peptides cannot be detected by conventional techniques. Comparison of CD spectra provided further support for the exclusive binding of copper(II) to the amino terminus of the octapeptide. No change of CD spectra can be recorded in the whole pH range from 5 to 11 supporting the existence of the same coordination mode in the species [$CuH_{-1}L$] and $[CuH_{-2}L]^-$. Moreover, this spectrum is very similar to that of the [$CuH_{-2}L$] species of the terminally free tetrapeptide NH_2-MKHM as it is shown by Figure 2. The addition of the second equivalent of copper(II) ion, however, drastically changes the CD spectra indicating the formation of another coordination environment. Figure 2 is used to compare the CD spectra of the high pH 1:1 (spectrum „a") and 2:1 („b") copper(II)-AAHAAAHG samples with those

of the $[CuH_{-2}L]$ species of NH_2-MKHM („c") and $[CuH_{-3}L]^-$ of Ac-MKHM („d") [25]. It is evident from this Figure that spectrum „a" resembles to that of „c" indicating the binding of copper(II) to the amino terminus of the octapeptide. On the other hand, the CD spectrum of the dinuclear species (spectrum „b") is in a good correlation with spectrum „e" which was obtained by the simple superposition of spectra „c" and „d". This is an unambiguous proof for the saturation of metal binding sites around both histidyl residues but the changes of EPR spectra provide further evidence. Well-resolved EPR spectra were recorded in the equimolar samples while a significant line-broadening is observed by the addition of the second equivalent of copper(II) ions supporting the existence of some magnetic interactions between the close copper(II) centres (Figures S3 and S4).

Table 2

Figure 2

It has already been discussed that the similar speciation of the copper(II) and nickel(II) complexes suggest the existence of similar coordination modes. This assumption was proved by the use of visible absorption, CD and ^{1}H NMR spectroscopic measurements on the nickel(II) containing systems. The yellow color and the diamagnetism of the high pH samples indicates the formation of square planar complexes which is characteristic for the nickel(II) complexes of all oligopeptides (see the absorption spectra in Figure S5). The ^{1}H NMR spectra of the species $[NiH_{-2}L]^-$ clearly indicate two sets of signals of the C(2) and C(5) protons of imidazole; one of them corresponds to a free imidazole (His7 site) while the other peaks are upfield shifted because imidazole-N donor is involved in (NH_2,$2N^-$,N_{im}) binding.

The spectral parameters of the major species calculated from the absorption and CD spectra are included in Table 2. The comparison of the spectroscopic data obtained for the nickel(II)-octapeptide complexes to those reported for the terminally free and protected tetrapeptides [15] led to the same conclusions as reported for copper(II) in the previous

paragraph. Both the absorption and CD spectra of the $[NiH_{-2}L]^-$ complex of the octapeptide are almost the same as those of the terminally free tetrapeptide (NH_2-MKHM) supporting the coordination of the first nickel(II) to the amino terminus. The binding of the second nickel(II) ion is much less favoured and it gives rise to the ($3N^-$,N_{im}) coordination mode around the His(7) binding site.

3.2. Speciation and structure of the copper(II), nickel(II) and zinc(II) complexes of the terminally free heptapeptide, AHAAAHG

The acid-base properties of the heptapeptide AHAAAHG are very similar to those of the octapeptide. The corresponding stability constants are collected in Table 3. It is clear from the comparison of Tables 1 and 3 that even the measured pK values of the two peptides are very similar. This is in good agreement with the expectations because the same protonation sites are present in similar environments. There is also a good correlation between the stoichiometries of the metal complexes. The corresponding speciation curves, however, reveal significant differences in the complex formation processes of the two peptides. Figures 3.a and 3.b are used to demonstrate the distribution of copper(II) ions among the various species at two different ratios, while the speciation of the equimolar zinc(II)-AHAAAHG samples are depicted in Figure 4. (The speciation of the corresponding nickel(II) complexes is shown by Figure S6 in the Supplement).

Table 3

Figure 3

Figure 4

Before the interpretation of the results it is important to clarify the major differences in the possible metal binding sites of the two peptides. Histidine is the second amino acid in the sequence of the heptapeptide, therefore the albumin-like binding is not possible. Former

studies on the metal complexes of GlyHis and AlaHis, however, revealed that these peptides are also effective complexing agents via the tridentate coordination of the (NH_2,N^-,N_{im}) binding sites [1,3,26]. Moreover, it was suggested that the metal ion promoted amide deprotonation of these peptides can occur not only in the copper(II) and nickel(II) complexes, but also for the corresponding zinc(II) containing systems [27-29]. The speciation curves suggest that all these interactions reported for the small dipeptides may also occur with the heptapeptide. The preferred tridentate coordination of the amino terminus and the presence of the other histidyl site, however, provides the chance for the existence of other coordination modes, too. The combined application of the potentiometric and various spectroscopic techniques made it possible to identify these coordination modes.

The comparison of Figures 1.a and 3.a led to a slightly surprising observation. The copper(II) binding affinity of the heptapeptide seems to be even higher than that of the octapeptide containing the albumin-like binding site. This statement can be justified by the comparison of the free copper(II) concentrations at pH 4.0: 27 % and 92 % for AHAAAHG and AAHAAAHG, respectively. On the other hand, this observation indicates well that the N-terminally free peptides with Xaa-His-.. sequence are also very effective metal binding ligands. Some recent studies provide further support for the enhanced metal binding ability of similar peptide sequences [30,31]. The formation of three major species can be seen in the equimolar samples of copper(II) and AHAAAHG (see Figure 3.a). Spectroscopic parameters of these complexes are collected in Table 4. The species $[CuL]^+$ predominates in the acidic pH range (pH = 3.5 to 5.5) and its absorption maxima supports the (NH_2,N^-,N_{im}) coordination mode. Its stoichiometry may correspond to the binding of the ligand without any extra deprotonation reaction via the coordination of terminal amino and one or two imidazole-N in the form of macrochelates. The absorption maxima of these macrochelates, however, generally observed at lower energies without CD activity. EPR parameters of the species also

support the tridentate coordination in the form of two fused chelate rings. It can be concluded from these data that the real stoichiometry of the species is $[CuL]^{+}$= $[CuH_{-1}L(H)]^{+}$ in which the amino terminus is tridentately coordinated while the other histidyl residue His(6) is still protonated. The pH range of deprotonation corresponds well to an imidazolium group and is accompanied with a significant blue shift of the absorption maxima suggesting the involvement of one more nitrogen atom in copper(II) binding. Similar conclusion can be drawn from the change of EPR spectra (Figures S7 and S8); in fact the EPR parameters change with a decrease of the $g_{||}$ and an increase of $A_{||}$, indicating the replacement of the equatorial water molecule with a stronger donor. On the other hand, the formation of $[CuH_{-1}L]$ from $[CuL]^{+}$does not have a significant effect on the CD spectra. All these information support the formation of a macrochelate with the involvement of the amino terminus and His(6) residue as it is shown by Scheme 2. It is clear from Figure 3.a that this species predominates in a very wide pH range (pH = 5.5 to 10.5) and the new base consuming process can be observed only at highly alkaline samples. It is also obvious from Table 4 that the formation of $[CuH_{-2}L]^{-}$ is accompanied with a further blue shift of absorption maxima and a characteristic change of CD spectra, while practically no change can be observed in the EPR spectra. Previous studies on the copper(II) complexes of GlyHis and related peptides came to the conclusion that the extra base consuming process comes from the deprotonation of the pyrrole type NH group of imidazole and the blue shift was explained by the formation of an imidazolato-bridged tetranuclear complex in which all coordination sites of copper(II) are saturated [32]. The formation of similar species were suggested in the nickel(II), and palladium(II) complexes, too [33]. The coordination sphere of the $[CuH_{-1}L]$ species of the heptapeptide is, however, saturated and the steric effects of the bulky heptapeptide also suppress the chance for oligomerization. The formation of mixed hydroxo complex is another explanation for the formation of $[CuH_{-2}L]^{-}$ but the changes of the absorption and circular

dichroism spectra contradict with this reaction. His(6) residue can, however, behave as another anchoring site of the molecule at high pH values. The partial rearrangement of copper(II) ions from the amino terminus to the internal histidyl site can result in the formation of another species with $[CuH_{-3}L]^{2-}$ stoichiometry with (N_{im},$3N^-$) coordination mode. The changes of absorption and CD spectra support this explanation, while the differences in the EPR parameters are too small to differentiate between the (NH_2,N^-,$2N_{im}$) and (N_{im},$3N^-$) coordination modes, especially if one of them is a favoured species. The well resolved EPR spectra, however, unambiguously support the existence of monomeric species under these conditions. Model calculations taking into account the stability constants reported for small peptides representing the two different coordination modes provided further support for the co-existence of the two different coordination modes. The distribution of copper(II) ions between two model peptides was calculated by using stability constants reported for the terminally free dipeptide GlyHis [26] and the terminally protected Ac-MetLysHisMet [25] mimicking the coordination environments around His(2) and His(6) respectively. It was found that copper(II) ions are exclusively bonded to the dipeptide around the physiological pH, but some 15 % of copper(II) is transformed to the 4N-coordinated species of the tetrapeptide at high pH. These calculations strongly support the existence of coordination isomers of the copper(II) complex of AHAAAHG at high pH values. The ratio of the two isomers is, however, not equivalent. The coordination at the amino terminus is favored over the internal histidyl site and this is further enhanced by the macrochelate as compared to the ratios obtained from the model calculations.

The comparison of Figures 1.b and 3.b reveals that the formation of dinuclear species is less favoured with the heptapeptide. The explanation of this observation comes from the macrochelate. The internal His(6) residue is involved in macrochelation in the mononuclear species and less available for binding of the second metal ion as compared to the free internal

histidine of the octapeptide. The changes of CD spectra in the presence of excess of copper(II) ions follow the same trends as reported for Ac-MKHM and related peptides, indicating the coordination of copper(II) at this histidyl site. Moreover, the bad resolution of EPR spectra of the 2:1 copper(II)-AHAAAHG samples at high pH provides further support for the formation of dinuclear copper(II) species.

Table 4

Scheme 2

The speciation of the corresponding nickel(II) complexes of AHAAAHG are very similar to the copper(II) containing systems (see Table 3). UV-visible spectra unambiguously prove that all nickel(II) containing species are square planar and diamagnetic supporting the existence of the same macrochelate as suggested for copper(II) in Scheme 2. ^{1}H NMR spectra of the nickel(II) complexes of AHAAAHG provided further support for the existence of this coordination mode. Proton resonances of the N-terminal Ala methyl groups occur at 1.27 ppm in the deprotonated free ligand at pH 9.37, while it is shifted to 0.96 ppm in the species $[NiH_{-1}L]$. This upfield shift is an unambiguous proof for the deprotonation and nickel(II) coordination of the first amide group. At the same time, the changes of imidazole protons indicate the metal binding of both His(2) and His(6) sites. The C(2) and C(5) protons of the two imidazole cannot be differentiated: two peaks can be observed at 6.95 and 7.67 ppm. There are, however, two sets of imidazole peaks in the corresponding nickel(II) complexes: at 6.23/7.36 and 6.88/8.01 ppm indicating the coordination of both imidazole in different environments.

It is clear from Table 4 that the formation of $[NiH_{-2}L]^{-}$ from $[NiH_{-1}L]$ is accompanied with a slight blue shift of the visible absorption spectra and a drastic change of CD parameters. These changes cannot be interpreted by the existence of two coordination isomers as described for copper(II) in the previous paragraphs. The formation of imidazolato-bridged

tetranuclear complexes in comparable concentration with the various 4N-coordinated mononuclear species can be responsible for these changes. It is also important to note that the formation of dinuclear nickel(II) complexes is very much shifted to the high pH range. As a consequence, nickel(II) hydroxide precipitate can be easily formed in these samples. To avoid precipitation spectra were recorded at 1.5:1 metal to ligand ratio but the co-existence of a series of various species is expected in these samples around pH 10.0. They include the mononuclear macrochelate, the hydroxo complex, the binding of nickel(II) at the His(6) site, the imidazolato bridged tetranuclear species and the dinuclear complex as the major species under these conditions.

The most striking difference in the complex formation processes of the octa- and heptapeptides was obtained for the zinc(II) containing systems. The potentiometric measurements clearly indicate the titration of an extra equivalent of base around pH 7.0, which can be attributed to the deprotonation and metal ion coordination of the first amide group in the same macrochelate as reported for copper(II) and nickel(II) (see Scheme 2) [27-29]. The binding of a second equivalent of zinc(II) is, however, not possible due to precipitation in the presence of excess of metal ion. No precipitation occurs in the equimolar samples supporting that the species $[ZnH_{-2}L]^{-}$ is a mixed hydroxo complex.

3.3. Studies on the formation of mixed metal complexes

The presence of dinuclear complexes in the copper(II) and nickel(II) containing systems provides the opportunity for the formation of mixed metal dinuclear species. The interactions with all three combinations of the metal ions were studied in the equimolar samples of two different metal ions and one of the peptides by spectroscopic studies.

It has already been described in Section 3.1 that the octapeptide AAHAAAHG has an outstanding affinity towards both copper(II) and nickel(II) ions, but the stability constants of

corresponding zinc(II) complexes are relatively low. As a consequence, the potentiometric titrations resulted in precipitation of zinc(II)-hydroxide in the mixed copper(II)-zinc(II) and nickel(II)-zinc(II)systems. The precipitation prevents the equilibrium analysis of these systems but the detection of mixed metal species can be possible by spectroscopic techniques. The results of spectroscopic studies, however, ruled out the formation of zinc(II) containing mixed species in detectable concentrations. In the case of the copper(II)-zinc(II)-AAHAAAHG system UV-visible, CD and EPR spectra were recorded by increasing pH. A complete agreement of the spectra of the ternary copper(II)-zinc(II) and binary copper(II) complexes was obtained by all three techniques. This observation is in accordance with the expectations because zinc(II) cannot promote amide deprotonation and coordination of this peptide at either His(3) or His(6) sites. Of course, these data do not rule out the presence of a zinc(II) containing species in very low concentration in which zinc(II) is monodentately coordinated at the imidazole of His(6) residue. This, however, can be only a minor species and cannot prevent the hydrolysis of zinc(II) by increasing pH.

The formation of mixed metal complexes were, however, unambiguously proved in the copper(II)-nickel(II)-AAHAAAHG system. There was also a slight precipitation of nickel(II) hydroxide in these systems preventing the determination of stability constants. These precipitates were, however, dissolved by high pH providing the opportunity for the quantitative evaluation of the spectra recorded in the mixed metal systems. ESI MS spectra of the mixed metal species were recorded in alkaline samples and the results are shown by Figure 5. The complete agreement of the isotopic distribution of the measured and calculated spectra provides an unambiguous proof for the predominance of the $[CuNiH_{-5}L]^{2-}$ mixed metal complex at high pH. It is clear from the visible (Figure S9) and CD spectra that only copper(II) ions are bonded in peptide complexes below pH 6.0 when the (NH_2,N^-,N^-,N_{im}) coordinated copper(II) complexes are completely formed. The characteristic changes of these

spectra by increasing pH, however, clearly show the binding of nickel(II) to the copper(II) containing species. On the contrary, the EPR spectra of the ternary copper(II)-nickel(II) and binary copper(II)-peptide systems are completely the same indicating the presence of a 4N-coordinated copper(II) ion at the amino terminus (Figure S10 and S11). This observation can be explained if the nickel(II) binding occurs only at the internal His(7) site in the form of ($3N^-$,N_{im}) binding mode, while the coordination environment of copper(II) remains unchanged in the whole pH range. The results of circular dichroism measurements strongly support this conclusion. CD spectra of the copper(II)-nickel((II)-AAHAAAHG samples are shown by Figure 6 at two different pH values (see spectra „c" and „d"). It can be seen that only copper(II) complexes are present in slightly acidic samples and the characteristic changes from nickel(II) coordination are observed in the alkaline samples. The spectra „a" and „b" are the CD spectra of model compounds containing the separated (NH_2,N^-,N^-,N_{im}) and ($3N^-$,N_{im}) coordination modes for copper(II) and nickel(II), respectively. It is evident from this Figure that the high pH CD spectrum of the mixed metal complex reflects the characteristics of copper(II) and nickel(II) coordinations at the amino terminus and the internal histidyl site, respectively.

Figure 5

Figure 6

It was thoroughly described in paragraph 3.2 that in the case of AHAAAHG all three metal ions, copper(II), nickel(II) and zinc(II) are able to induce deprotonation and metal ion coordination of the amide group between Ala(1) and His(2) residues. This may suggest the formation of mixed metal complexes containing zinc(II) and one of the other two metal ions. The experimental evidence, however, does not support this expectation. The formation of hydoxide precipitates was observed in both the copper(II)-zinc(II) and nickel(II)-zinc(II) systems in the slightly alkaline samples and any changes in the UV-visible, CD or EPR

spectra of the samples were not observed as compared to those of the binary copper(II) or nickel(II) complexes. The spectroscopic measurements revealed that the formation of mixed metal species is less favoured even in the copper(II)-nickel(II)-AHAAAHG system as compared to the octapeptide. The copper(II) containing binary species ($[CuL]^+$ and $[CuH_{-1}L]$) of the heptapeptide are formed by pH 4.0 but the mixed metal species are present only above pH 9.0, while these species were formed by pH 8.0 with the octapeptide. This difference in the relative stabilities of the mixed metal complexes comes from the macrochelation with the heptapeptide. The internal His(7) residue of the octapeptide is free and easily available for nickel(II) binding, while the His(6) of the heptapeptide is involved in copper(II) coordination. This binding is able to suppress but does not prevent the coordination of nickel(II) ions at high pH values. Figure 7 is used to demonstrate the high pH CD spectra of the copper(II)-nickel(II)-AHAAAHG system (spectra „c"). CD spectra of the species $[CuL]^+$ of AHAAAHG (a) and $[NiH_{-3}L]^-$ of Ac-MKHM containing the ($3N^-$,N_{im}) coordination mode (b) are also plotted for comparison. These data strongly support that the partial binding of nickel(II) occurs at the His(6) site and the preceding three amide groups while the coordination environment of copper(II) is the same in the ternary and binary species. The EPR spectra provide further support for this conclusion, because the EPR spectra of copper(II) containing samples does not change upon addition of nickel(II) ions.

Figure 7

4. Conclusion

This study on the copper(II), nickel(II) and zinc(II) complexes of the terminally free peptides AHAAAHG and AAHAAAHG provides a good chance to compare the metal binding affinity and selectivity of three major coordination modes of peptides. The tridentate (NH_2,N^-,N_{im})

and tetradentate (NH_2,N^-,N^-,N_{im}) coordinations can be formed at the amino termini of the hepta- and octapeptides, respectively, while the tetradentate ($3N^-$,N_{im}) coordination mode can be formed with the internal histidyl sites of both peptides (His(6) for AHAAAHG and His(7) for AAHAAAHG). The results unambiguously prove that the donor sites with the involvement of the amino termini are more effective complexing agents than the internal histidyl sites. On the other hand, the (NH_2,N^-,N^-,N_{im}) binding mode seems to be rather selective for copper(II) and nickel(II) binding but it has only low affinity for zinc(II) coordination. On the contrary, the tridentate (NH_2,N^-,N_{im}) coordination of the heptapeptide can effectively bind all three metal ions and the stability of these complexes can be further enhanced via macrochelation of another histidyl residue. The internal histidyl residues can also be anchoring sites for copper(II) and nickel(II) binding and promote the deprotonation of amide nitrogens preceding the imidazole-N donor functions. The overall thermodynamic stabilities of these species are, however, always lower than those formed with the N-terminal sites.

It is also an important conclusion of this study that the presence of well separated histidyl residues in peptides creates a great chance for the formation of dinuclear and/or mixed metal complexes. The significant differences in the thermodynamic stabilities of the various coordination modes, however, result in the preference of the N-terminally coordinated species, but the coexistence of the (NH_2,N^-,N_{im}) and ($3N^-$,N_{im}) coordination modes can also occur as it was found for the copper(II)-AHAAAHG system. The results also proved that in the mixed metal species always copper(II) ions saturate the N-terminal sites and nickel(II) coordination is shifted to the internal histidyl residues. This conclusion is slightly different from those reported for the mixed metal copper(II)-nickel(II) species of the peptide fragments of prion protein [19]. In the latter system the addition of nickel(II) ions to the copper(II) complexes was able to redistribute copper(II) among the available binding sites. The peptide

fragments of prion proteins, however, contain only internal histidyl sites of which the metal binding affinities are well comparable. The distribution of metal ions among the binding sites with significant difference in stability, however, will follow the trends which correspond to the thermodynamic stabilities of the species.

5. Abbreviations

CD – circular dichroism

UV-visible (UV-Vis) – ultraviolet-visible absorption spectroscopy

MS – mass spectra

Fmoc – N-fluorenylmethoxycarbonyl

DMF – dimethyl formamide

TFA – trifluoracetic acid

Trt - trytil

Acknowledgements

The authors thank OTKA 72956 for financial support. The research was also supported by EU and co-financed by the European Social Fund under the project ENVIKUT (TAMOP-4.2.2.A-11/1/KONV-2012-0043 and TAMOP-4.2.2.B-10/1-2010-0024).

References

[1] H. Kozlowski, W. Bal, M. Dyba, T. Kowalik-Jankowska, Coord. Chem. Rev., 184 (1999) 319-346.

[2] H. Kozlowski, T. Kowalik-Jankowska, M. Jezowska-Bojczuk, Coord. Chem. Rev., 249 (2005) 2323-2334.

[3] I. Sóvágó, K. Ősz, Dalton Trans., (2006) 3841-3854.

[4] D. Witkowska, M. Rowinska-Zyrek, G. Valensin, H. Kozlowski, Coord. Chem. Rev., 256 (2012) 133-148.

[5] G. Arena, D. La Mendola, G. Pappalardo, I. Sóvágó, E. Rizzarelli, Coord. Chem. Rev., 256 (2012) 2202-2218.

[6] I. Sóvágó, C. Kállay, K. Várnagy, Coord. Chem. Rev., 256 (2012) 2225-2233.

[7] N. Camerman, A. Camerman, B. Sarkar, Can. J. Chem., 54 (1976) 1309-1316.

[8] C. Kállay, K. Várnagy, G. Malandrinos, N. Hadjiliadis, D. Sanna, I. Sóvágó, Dalton Trans., (2006) 4545-4552.

[9] A. Jancsó, A. Kolozsi, B. Gyurcsik, N.V. Nagy, T. Gajda, J. Inorg. Biochem., 103 (2009) 1634-1643.

[10] S. Timári, C. Kállay, K. Ősz, I. Sóvágó, K. Várnagy, Dalton Trans., (2009) 1962-1971.

[11] D. La Mendola, A. Magri, A.M. Santoro, V. G. Nicoletti, E. Rizzarelli, J. Inorg. Biochem., 111 (2012) 59-69.

[12] D. Valensin, M. Luczkowski, F.M. Mancini, A. Legowska, E. Gaggelli, G. Valensin, K. Rolka, H. Kozlowski, Dalton Trans., (2004) 1284-1293.

[13] G. Di Natale, K. Ősz, Z. Nagy, D. Sanna, G. Micera, G. Pappalardo, I. Sóvágó, E. Rizzarelli, Inorg. Chem., 48 (2009) 4239-4250.

[14] C. A. Damente, K. Ősz, Z. Nagy, G. Pappalardo, G. Grasso, G. Impellizzeri, E. Rizzarelli, I. Sóvágó, Inorg. Chem., 47 (2008) 9669-9683.

[15] I. Turi, C. Kállay, D. Szikszai, G. Pappalardo, G. Di Natale, P. De Bona, E. Rizzarelli, I. Sóvágó, J. Inorg. Biochem., 104 (2010) 885-891.

[16] G. Arena, G. Pappalardo, I. Sóvágó, E. Rizzarelli, Coord. Chem. Rev., 256 (2012) 3-12.

[17] S. Rajkovic, C. Kállay, R. Serényi, G. Malandrinos, N. Hadjiliadis, D. Sanna, I. Sóvágó, Dalton Trans., (2008) 5059-5071.

[18] E. D. Walter, D. J. Stevens, M.P. Visconte, G.L. Millhauser, J. Am. Chem. Soc., 129 (2007) 15440-15441.

[19] V. Jószai, I. Turi, C. Kállay, G. Pappalardo, G. Di Natale, E. Rizzarelli, I. Sóvágó, J. Inorg. Biochem., 112 (2012) 17-24.

[20] É. Józsa, K. Ősz, C. Kállay, P. De Bona, C.A. Damante, G. Pappalardo, E. Rizzarelli, I. Sóvágó, Dalton Trans., 39 (2010) 7046-7053.

[21] C.A. Damante, K. Ősz, Z. Nagy, G. Grasso, G. Pappalardo, E. Rizzarelli, I. sóvágó, Inorg. Chem., 50 (2011) 5342-5350.

[22] C. Kállay, K. Ősz, A. Dávid, Z. Valastyán, G. Malandrinos, N. Hadjiliadis, I. Sóvágó, Dalton Trans., (2007) 4040-4047.

[23] C. Kállay, K. Várnagy, G. Malandrinos, N. Hadjiliadis, D. Sanna, I. Sóvágó, Inorg. Chim. Acta, 362 (2009) 935-945.

[24] P.G. Daniele, P. Amico, G. Ostacoli, M. Marzona, Annali di Chimica, 73 (1983) 299-313.

[25] V. Jószai, Z. Nagy, K. Ősz, D. Sanna, G. Di Natale, D. La Mendola, G. Pappalardo, E. Rizzarelli, I. Sóvágó, J. Inorg. Biochem., 100, (2006) 1399-1409.

[26] I. Sóvágó, E. Farkas and A. Gergely, J. Chem. Soc., Dalton Trans.,(1982) 2159-2163.

[27] E. Farkas, I. Sóvágó and A. Gergely, J. Chem. Soc., Dalton Trans., (1983) 1545-1551.

[28] M.J.A. Rainer, B.M. Rode, Inorg. Chim. Acta, 93 (1984) 109-115.

[29] D.L. Rabenstein, S.A. Daignault, A.A. Isab, A.P. Arnold and M.M. Shoukry, J. Am. Chem. Soc.,107 (1985) 6435-6439.

[30] C. Hureau, H. Eury, R. Guillot, C. Bijani, S. Sayen, P.L. Solari, E. Guillon, P. Faller, P. Dorlet, Chem. Eur. J., 17 (2011) 10151-10160.

[31] A. Trapaidze, C. Hureau, W. Bal, M. Winterhalter, P. Faller, J. Biol. Inorg. Chem., 17 (2012) 37-47.

[32] P.J. Morris, R.B. Martin, J. Inorg. Nucl. Chem., 33 (1971) 2913-2918.

[33] M. Wienken, B. Lippert, E. Zangrando, L. Randaccio, Inorg. Chem., 31 (1992) 1983-1985.

Table 1. Protonation and stability constants (log β_{pqr}) of the metal complexes of the octapeptide AAHAAAHG

(T = 298 K, I = 0.2 M, KCl, standard deviations are in parenthesis)

Species	log β_{pqr}	pK	
[HL]	7.97(1)	7.97	
$[H_2L]^+$	14.85(1)	6.88	
$[H_3L]^{2+}$	20.99(2)	6.14	
$[H_4L]^{3+}$	24.11(3)	3.12	
	Cu(II)	Ni(II)	Zn(II)
$[MHL]^{2+}$	14.48(3)	–	11.50(2)
$[ML]^+$	–	–	4.50(3)
$[MH_{-1}L]$	6.06(1)	–0.30(9)	–2.92(1)
$[MH_{-2}L]^-$	–0.88(4)	–7.04(6)	–
$[M_2H_{-2}L]^+$	3.67(3)	–3.36(11)	–
$[M_2H_{-3}L]$	–2.56(3)	–11.93(24)	–
$[M_2H_{-4}L]^-$	–9.39(2)	–20.33(15)	–
$[M_2H_{-5}L]^{2-}$	–19.02(2)	–29.18(5)	–
pK(1)	–	–	7.00
pK(2)	–	–	7.42
pK(3)	6.94	6.74	–

Table 2. Spectroscopic data of the major species formed in the copper(II)- and nickel(II)-AAHAAAHG system

Species	λ/ε (nm/$M^{-1}cm^{-1}$)	$\lambda/\Delta\varepsilon$ (nm/$M^{-1}cm^{-1}$)	$g_{\|\|}/A_{\|\|}(10^{-4}$ $cm^{-1})$
$[CuH_{-1}L]$	522/94	306/1.18	2.188/201
		483/0.43	
		565/–0.56	
$[CuH_{-2}L]^{-}$	525/108	305/1.28	2.186/202
		485/0.48	
		569/–0.61	
$[Cu_2H_{-4}L]^{-}$	528/100	305/0.63	
		492/0.19	
		570/–0.16	
$[Cu_2H_{-5}L]^{2-}$	524/107	310/0.79	
		545/–0.35	
		637/0.30	
$[NiH_{-2}L]^{-}$	422/138	260/2.15	
		410/1.48	
		474/–2.26	
$[Ni_2H_{-5}L]^{2-}$	424/124	398/0.23	
		468/–0.94	

Table 3. Protonation and stability constants (log β_{pqr}) of the metal complexes of AHAAAHG (T = 298 K, I = 0.2 M, KCl, standard deviations are in parenthesis)

Species	log β_{pqr}	pK	
[HL]	7.94(1)	7.94	
$[H_2L]^{+}$	14.77(1)	6.83	
$[H_3L]^{2+}$	20.84(2)	6.07	
$[H_4L]^{3+}$	23.95(3)	3.11	
	Cu(II)	Ni(II)	Zn(II)
$[MHL]^{2+}$	15.73(3)	-	11.42(2)
$[ML]^{+}$	12.73(3)	6.31(2)	4.65(2)
$[MH_{-1}L]$	7.37(4)	0.73(3)	–2.08(1)
$[MH_{-2}L]^{-}$	–3.11(5)	–9.36(5)	–11.40(3)
$[M_2H_{-2}L]^{+}$	3.49(2)	–4.74(1)	–
$[M_2H_{-3}L]$	–2.74(2)	–14.40(1)	–
$[M_2H_{-4}L]^{-}$	–10.75(6)	–23.13(2)	–
$[M_2H_{-5}L]^{2-}$	–19.86(7)	–32.22(6)	–
pK(1)	3.00	–	6.77
pK(2)	5.36	5.58	6.73
pK(3)	10.48	10.09	9.32

Table 4. Spectroscopic data of the major species formed in the copper(II)- and nickel-AHAAAHG system

Species	λ/ε (nm/$M^{-1}cm^{-1}$)	λ/Δε (nm/$M^{-1}cm^{-1}$)	$g_{\|\|}/A_{\|\|}(10^{-4}$ $cm^{-1})$
$[CuL]^{+}$	594/60	341/0.08	2.230/196
		514/–0.04	
		617/0.13	
$[CuH_{-1}L]$	567/86	334/0.11	2.212/202
		533/–0.13	
		637/0.30	
$[CuH_{-2}L]^{-}$	554/92	322/0.23	2.212/202
		510/–0.30	
		625/0.28	
$[Cu_2H_{-3}L]$	573/77	310/–0.15	
		625/0.15	
$[Cu_2H_{-4}L]^{-}$	573/89	318/0.05	
		486/–0.32	
		620/0.40	
$[Cu_2H_{-5}L]^{2-}$	542/91	318/0.52	
		485/–0.60	
		615/0.46	
$[NiH_{-1}L]$	443/106	493/0.36	
$[NiH_{-2}L]^{-}$	441/152	470/–1.60	
$[Ni_2H_{-5}L]^{2-}$	436/173	417/–0.58	
		532/0.19	

Legends to Figures

Figure 1

Species distribution of the complexes formed in the copper(II)-AAHAAAHG system at 1:1 (a) and 2:1 (b) ratios. (c_L = 2 mM)

Figure 2

CD spectra of the high pH samples recorded in 1:1 (a) and 2:1 (b) ratios in the copper(II)-AAHAAAHG system. CD spectra of $[CuH_{-2}L]$ species of the N-terminally free tetrapeptide NH_2-MKHM (c) and $[CuH_{-3}L]^-$ of the N-terminalyl acylated peptide Ac-MKHM (d) [15,19]. Spectrum (e) is calculated by the superposition of spectra (c) and (d).

Figure 3

Species distribution of the complexes formed in the copper(II)-AHAAAHG system at 1:1 (a) and 2:1 (b) ratios. (c_L = 2 mM)

Figure 4

Species distribution of the complexes formed in the zinc(II)-AHAAAHG system at 1:1 ratio. (c_L = 2 mM)

Figure 5

Measured (up) and simulated (down) ESI-MS spectra of the mixed metal complex $[CuNiH_{-5}L]^{2-}$ of the octapeptide AAHAAAHG at pH=10.3; at Cu(II):Ni(II):L = 0.9:0.9:1 ratio (c_L = 1×10^{-4} M).

Figure 6

CD spectra of the equimolar copper(II)-nickel((II)-AAHAAAHG samples at pH 5.08 (c) and 11.00 (d). Spectrum (a) corresponds to the (NH_2,N^-,N^-,N_{im}) coordinated species of the copper(II)-NH_2-MKHM system, while (b) represents the CD spectrum of the ($3N^-$,N_{im}) coordinated nickel(II) complex of Ac-MKHM [15,19].

Figure 7

CD spectra (c) of the equimolar copper(II)-nickel(II)-AHAAAHG samples at pH 11.48. Spectrum (a) corresponds to the tridentately coordinated species $[CuL]^+$ of AHAAAHG and spectrum (b) represents the CD spectrum of the ($3N^-$,N_{im}) coordinated nickel(II) complex of Ac-MKHM.

Scheme 1

The major coordination modes of histidine containing peptides:

(NH_2,N^-,N^-,N_{im}) (a), (N^-,N^-,N^-,N_{im}) (b) and (NH_2,N^-,N_{im}) (c).

Scheme 2

Coordination mode of the major species $[CuH_{-1}L]$ formed in the copper(II)-AHAAAHG system.

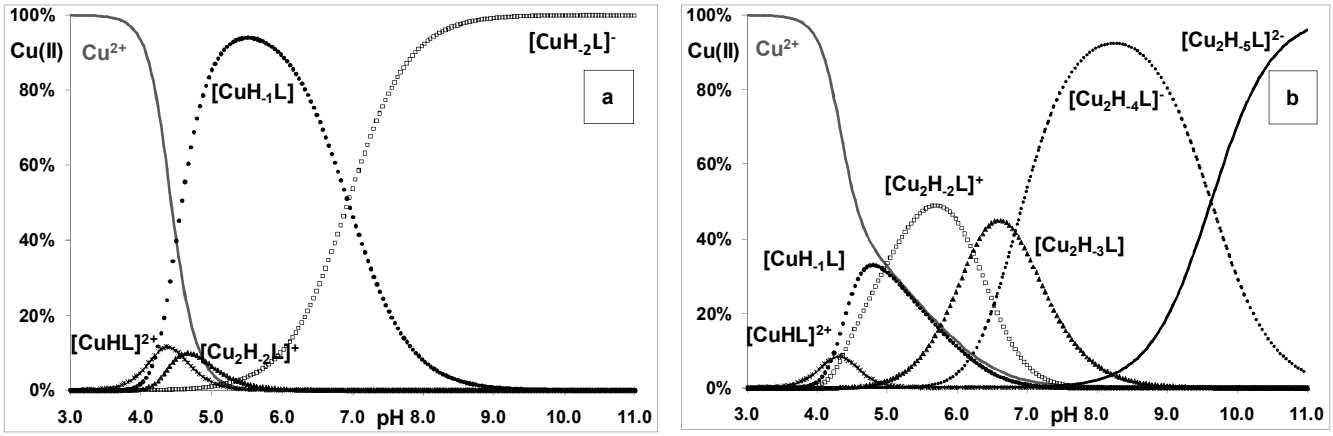
100%
Cu(II)
Cu2+
80%
60%
40%
20%
0%
[CuH-1L]
[CuH-2L]-
a
[CuHL]2+
[Cu2H-2L]+
3.0
4.0
5.0
6.0
7.0
pH
8.0
9.0
10.0
11.0
100%
Cu(II)
Cu2+
80%
60%
40%
20%
0%
[Cu2H-5L]2-
[Cu2H-4L]-
b
[Cu2H-2L]+
[Cu2H-3L]
[CuH-1L]
[CuHL]2+
3.0
4.0
5.0
6.0
7.0
pH
8.0
9.0
10.0
11.0

Figure 1

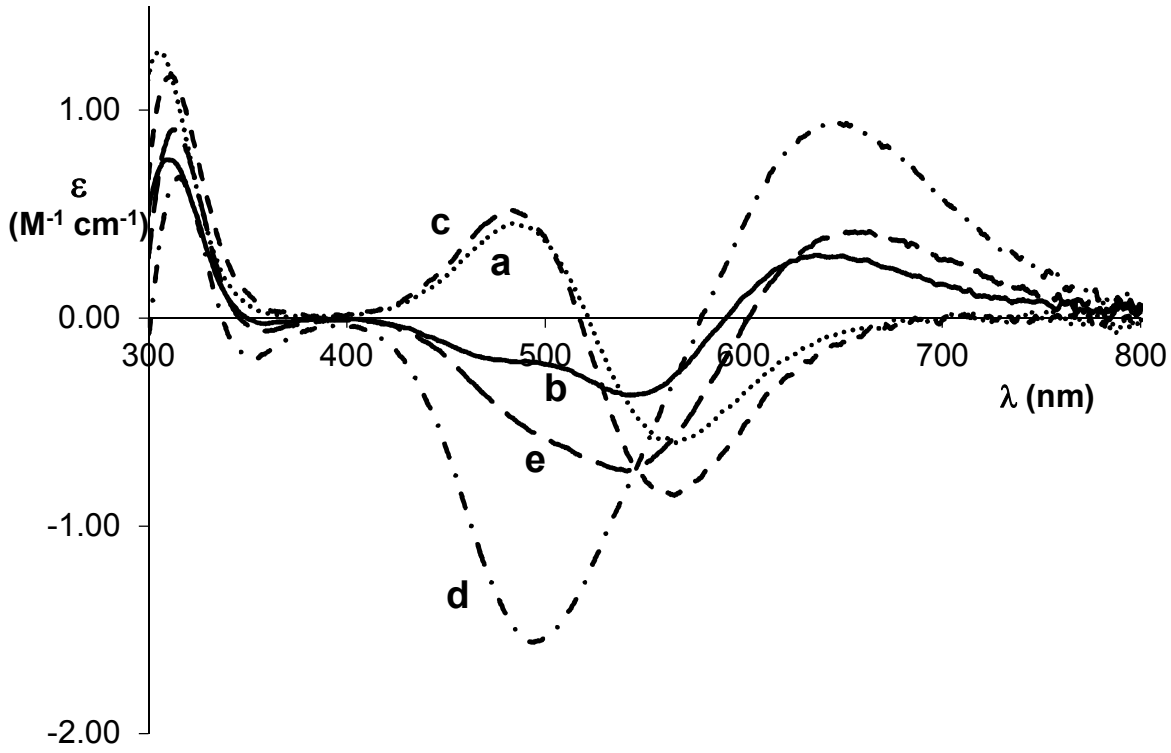

Figure 2

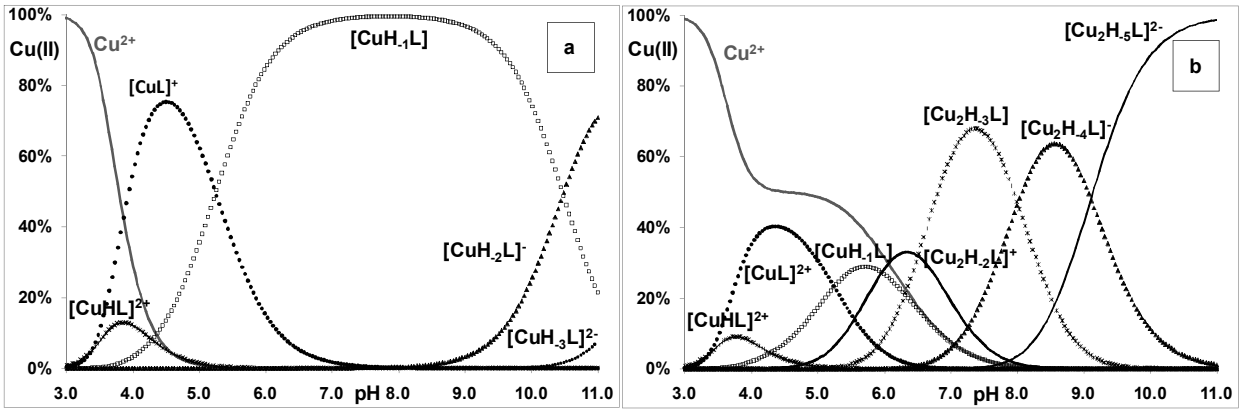
100%
Cu(II)
80%
60%
40%
20%
0%
Cu2+
[CuL]+
[CuH-1L]
[CuH-2L]-
[CuHL]2+
[CuH-3L]2-
a
3.0
4.0
5.0
6.0
7.0
pH
8.0
9.0
10.0
11.0
100%
Cu(II)
80%
60%
40%
20%
0%
Cu2+
[Cu2H-5L]2-
b
[Cu2H-3L]
[Cu2H-4L]-
[CuH-1L]
[CuL]2+
[Cu2H-2L]+
[CuHL]2+
3.0
4.0
5.0
6.0
7.0
pH
8.0
9.0
10.0
11.0

Figure 3

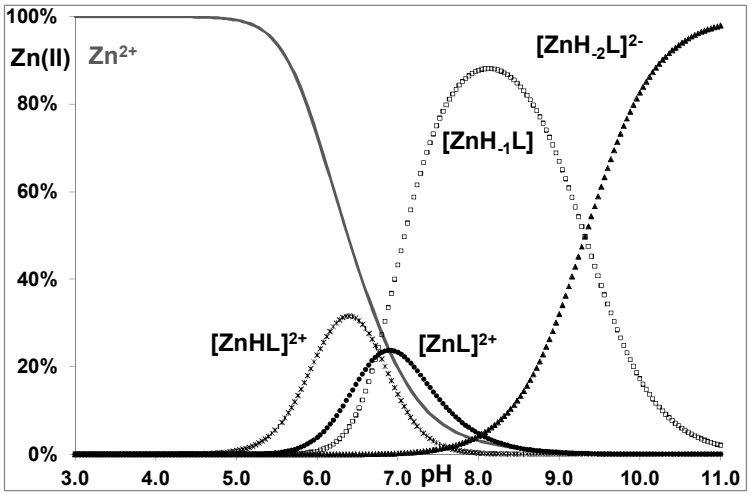
100%
Zn(II)
Zn2+
80%
60%
40%
20%
0%
[ZnH-2L]2-
[ZnH-1L]
[ZnHL]2+
[ZnL]2+
3.0
4.0
5.0
6.0
7.0
pH
8.0
9.0
10.0
11.0

Figure 4

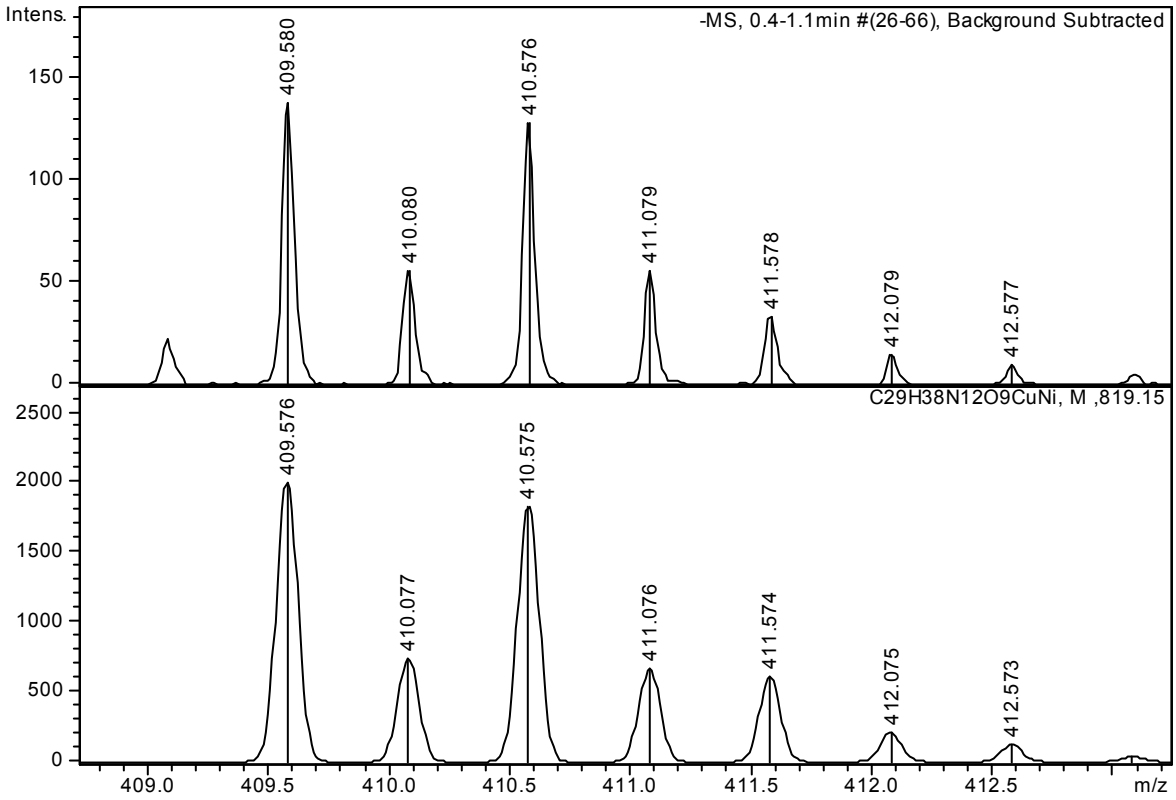
Intens.
-MS, 0.4-1.1min #(26-66), Background Subtracted
409.580
410.576
410.080
411.079
411.578
412.079
412.577
C29H38N12O9CuNi, M ,819.15
409.576
410.575
410.077
411.076
411.574
412.075
412.573
m/z

Figure 5

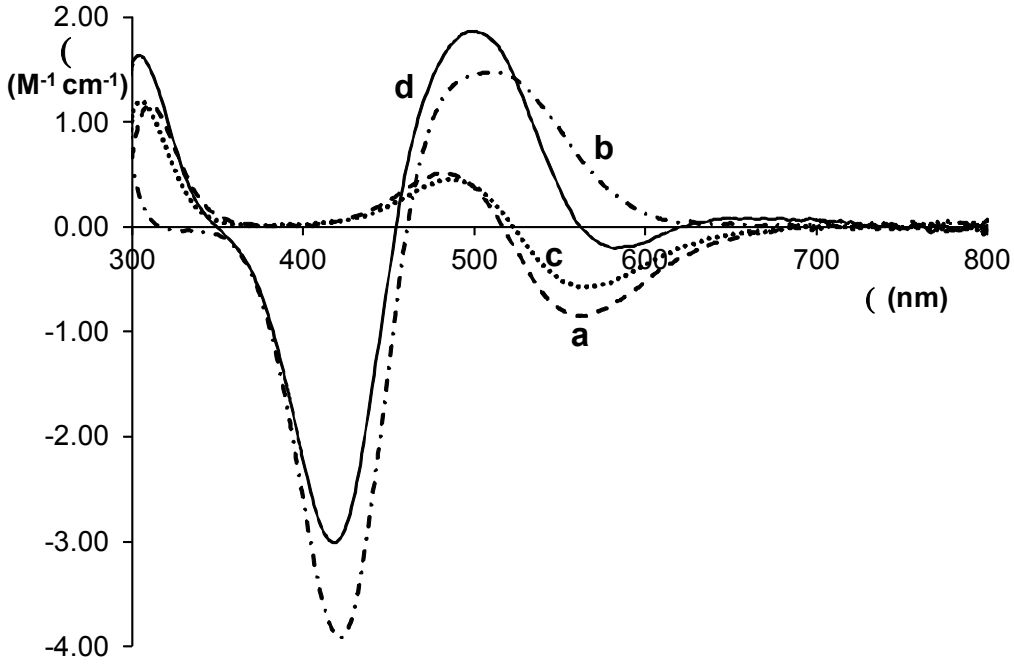
2.00
(
(M-1 cm-1)
1.00
0.00
-1.00
-2.00
-3.00
-4.00
300
400
500
600
700
800
((nm)
d
b
c
a

Figure 6

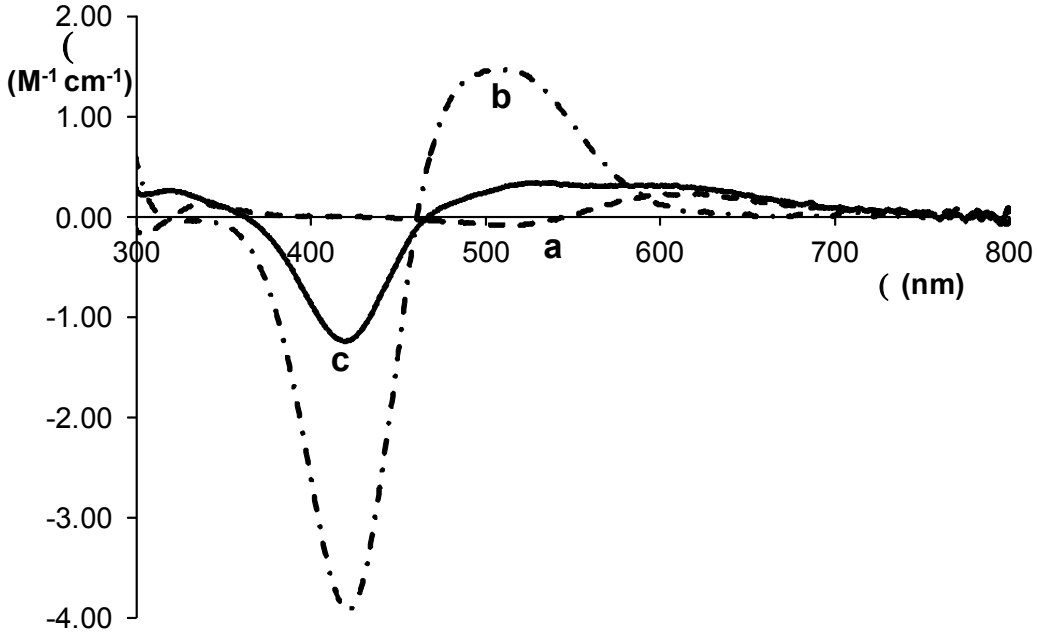

Figure 7

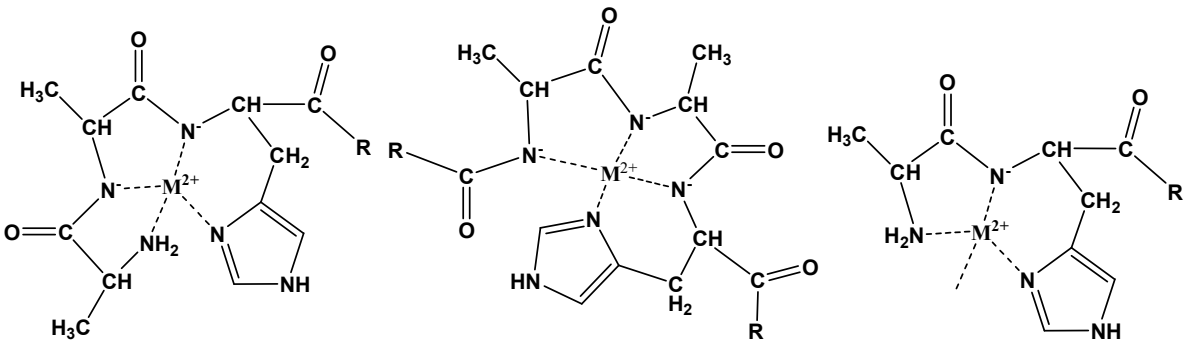

a **b** **c**

Scheme 1

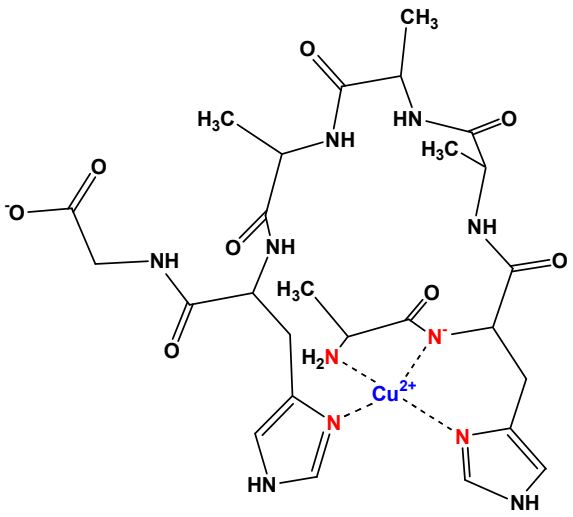

Scheme 2